European Thyroid Journal (2025) 14 e240137
https://doi.org/10.1530/ETJ-24-0137

Received 5 May 2024
Accepted 28 May 2025
Available online 28 May 2025
Version of Record published 12 June 2025

RESEARCH

Potential of bone marrow mesenchymal stem cells in iodine-induced autoimmune thyroiditis therapy

Xun Liu[1], Likun Cui[2], Jianwei Dong[3], Jiancong Ren[3], Dongdong Xu[3], Yanshuo Han[4,5] and Jian Zhang[3]

[1]Department of General Surgery, Shengjing Hospital of China Medical University, Shenyang, China
[2]Department of Ultrasound, Sichuan Clinical Research Center for Cancer, Sichuan Cancer Hospital & Institute, Sichuan Cancer Center, University of Electronic Science and Technology of China, Chengdu, China.
[3]Department of Vascular & Thyroid Surgery, The First Hospital of China Medical University, Shenyang, China
[4]Department of Vascular Surgery, Central Hospital of Dalian University of Technology, Dalian, China
[5]School of Chemical Engineering, Ocean Technology and Life Science, Dalian University of Technology, Panjin, China

Correspondence should be addressed to J Zhang: jianzhang@cmu.edu.cn

Abstract

Objective: Hashimoto's thyroiditis (HT) is a prevalent autoimmune disease without a cure. Mesenchymal stem cells (MSCs) may offer the opportunity to improve autoimmune thyroiditis.

Methods: We replicated the pathogenic factors of HT and established a stable autoimmune thyroiditis model in NOD.H-2^{h4} mice by administering iodine for 12 weeks. We used orthotopic injection to transplant bone MSCs (BMSCs) into the thyroid. Immunohistochemistry, enzyme-linked immunosorbent assay, flow cytometry, and hematoxylin and eosin and immunofluorescence staining were used to evaluate the effects of cell transplantation.

Results: Orthotopic BMSC transplantation decreased serum thyroglobulin antibody and caspase 3 levels; increased proliferating cell nuclear antigen levels; decreased $CD4^+/CD3^+$ T cells, Th1/Th2, and Th17/Treg ratios; decreased TNF-alpha (a proinflammatory cytokine) and interferon-gamma levels; and increased transforming growth factor-beta and interleukin-10 levels. In addition, it increased CD90/S100A4 and CD90/TTF-1 co-expression.

Conclusion: Orthotopic BMSC transplantation improved the inflammatory environment by regulating the secretion of anti-inflammatory cytokines, promoting regeneration, and reducing apoptosis in the thyroid tissue. Bone marrow-derived stem cells inhibited T cell activation, maintained a balance between T cell subpopulation ratios, and halted thyroiditis progression. Finally, transplanted BMSCs could transform into fibroblasts and thyroid cells. This study elucidated the pathogenesis of HT and provided evidence supporting the potential of MSCs in HT treatments.

Keywords: NOD.H-2^{h4} mice; autoimmune thyroiditis; bone marrow mesenchymal stem cells; mesenchymal stem cell transplantation

Introduction

Hashimoto's thyroiditis (HT) is an autoimmune condition characterized by chronic inflammatory cell infiltration and impaired thyroid function resulting from a faulty immune response. HT has gained attention owing to its increasing incidence and close relationship with papillary thyroid carcinoma (1, 2); however, its pathogenesis is unknown. Infection, mental dysfunction, excessive iodine intake, and drug abuse are potential pathogenic factors of HT (3). In China, iodine supplementation is a significant risk factor for HT (1, 4). Current treatments for HT are ineffective; oral administration of synthetic levothyroxine only

Published by Bioscientifica Ltd.
https://etj.bioscientifica.com

European Thyroid Journal (2025) **14** e240137
https://doi.org/10.1530/ETJ-24-0137

regulates thyroid function and alleviates symptoms (2). Moreover, HT lasts several years and develops into hypothyroidism, affecting patients' quality of life.

Mesenchymal stem cells (MSCs) originate in the embryonic mesoderm and are highly capable of regeneration, multilineage differentiation potential, and immunomodulation capacity (5, 6, 7, 8). The use of MSCs in immunoregulatory therapy is advancing toward phase II and III clinical trials for several autoimmune conditions, including multiple sclerosis, Crohn's disease, graft-versus-host disease, and refractory rheumatoid arthritis (9, 10, 11, 12). The therapeutic effectiveness of MSCs has been studied in various animal disease models, including asthma, rheumatoid arthritis, systemic lupus erythematosus, autoimmune colitis, meningitis, and myasthenia (13, 14, 15, 16). However, preclinical and clinical trials of MSCs in HT treatment are limited. Moreover, previous animal models established using the experimental autoimmune thyroiditis (EAT) method do not adequately simulate the pathogenic process, and MSC administration through caudal vein transplantation requires repeated injections, resulting in poor therapeutic efficacy (17, 18).

In this study, we modeled the natural HT pathophysiology to examine the beneficial effects of bone marrow MSCs (BMSCs). We replicated the pathogenic factors of HT and established a stable autoimmune thyroiditis model in NOD.H-2^{h4} mice by administering iodine for 12 weeks. Orthotopic transplantation of BMSCs was employed for treating autoimmune thyroiditis. Therapeutic effectiveness was assessed through alterations in thyroid histology, infiltration of immune cells, the performance of immunoregulation, and the potential for tissue regeneration after the transplantation of BMSCs. Our findings provide evidence supporting the potential of MSCs in HT treatment.

Materials and methods

Animals

NOD.H-2^{h4} mice were purchased from Jackson Laboratories (USA) and bred at the Animal Experimental Center of China Medical University, ensuring specific pathogen-free conditions. The mice were provided unrestricted access to food and water. The implemented experimental protocols and animal husbandry procedures were approved by the Institutional Animal Care and Use Committee at China Medical University (grant number 2018095).

Isolation and identification of BMSCs

Bone marrow-derived stem cells were isolated from five 3- to 4-week-old male NOD.H-2^{h4} mice. Mice were anesthetized with 3% isoflurane inhalation for induction and 1% for maintenance; after maintenance, mice were sacrificed by cervical dislocation. The bilateral femur and tibia were immediately removed and the metaphysis was cut off to access the bone cavity. The bone marrow within the cavity was flushed out with several rounds of phosphate-buffered saline (PBS) using a sterile syringe. The mixture was centrifuged at 111.8 ***g*** for 5 min at 4°C. The resulting cell pellets were resuspended in 5 mL Dulbecco's modified Eagle medium (DMEM; Hyclone, USA) supplemented with 10% fetal bovine serum (FBS; Gibco, USA) and 100 U/mL penicillin/streptomycin (1%) (Invitrogen, USA). The cell suspension was inoculated in a plastic culture flask. The medium was changed 24 h after incubation and then every 48 h. Bone marrow-derived stem cells were cultured for 10–14 days to achieve 80–90% confluence. The cells were then digested with trypsin and passaged for subsequent experiments.

Passage-1 cells were collected as described above to identify BMSC biomarkers. Cells were incubated with 1 μL anti-CD34 (1:100; Cat#AF6518, RD, USA), anti-CD90 (1:100; Cat#sc-53456, Santa Cruz, USA), anti-CD73 (1:100; Cat#AF4488, RD), or anti-CD105 (1:100; Cat#AF1320, RD) for 30 min at 20°C. After washing with PBS, the cells were stained using an Alexa Fluor® 488-conjugated fluorescent antibody (1:1,000; Cat#ab150177, Abcam, UK) for 30 min at room temperature. Blank controls were prepared using unstained cells. After washing, flow cytometry was used to identify BMSC specific markers.

The differentiation ability of BMSCs was validated using chondrogenic, osteogenic, and adipogenic induction protocols. These protocols were based on previous studies with minor adjustments (19). Passage-1 BMSCs were cultured in 6-well culture plates (5×10^5 cells per well) until 90% confluence. For adipocytes, cells were differentiated in DMEM with 10% FBS, 10^{-6} M dexamethasone, 0.5 μM 3-isobutyl-1-methylxanthine, and 10 ng/mL insulin. For osteoblasts, cells were differentiated in DMEM with 10% FBS, 10^{-7} M dexamethasone, 10 mM β-glycerol phosphate, and 50 μM ascorbate-2-phosphate. For chondrocytes, cells were differentiated in DMEM with 10% FBS, 10^{-7} M dexamethasone, 1% insulin transferrin sodium, 50 μM ascorbate-2-phosphate, 50 μg/mL proline, 1 mM sodium pyruvate, and 20 ng/mL transforming growth factor-beta 3 (TGF-β3).

Hashimoto's thyroiditis model development and BMSC transplantation

Iodine treatment was utilized to create a model of autoimmune thyroiditis in NOD.H-2^{h4} mice. Forty 6–8-week-old male mice (approximately 20 g) were randomly split into four groups (n = 10). The control group was provided sterilized water for 12 weeks. The treatment groups were given sterilized water with 0.05% sodium iodide (1,000 times the normal intake)

European Thyroid Journal (2025) **14** e240137
https://doi.org/10.1530/ETJ-24-0137

for 8, 12, and 16 weeks. At the end of the treatment period, the thyroid tissue was removed and the level of inflammatory cell infiltration was evaluated using hematoxylin and eosin (H and E) staining.

Two mice (model and control without thyroiditis) were chosen to confirm the efficacy of orthotopic transplantation of stem cells. The injection protocols were as follows: passage-1 BMSCs were harvested and reconstituted in 5 mL serum-free DMEM supplemented with 10 μL CM-Dil (1 mg/mL in dimethyl sulfoxide; Cat#C7000, Invitrogen). For transplantation, cells were resuspended in PBS (2×10^5 cells/mL) after incubation at 37°C for 5 min and chilled at 4°C for 15 min. After anesthesia, the method of anesthesia as described above, a blunt cut in the anterior tracheal muscle exposed the trachea and thyroid glands. The cell suspension (4 μL) was injected into the lower pole of the mouse thyroid glands using a pipette and gun tip connected to a 31-G sterile needle until the glands slightly swelled (Fig. 1A). The control mouse was injected with 4 μL PBS. The presence of BMSCs in the thyroid glands was verified 1 day after injection; paraffin-embedded sections were prepared and cells were examined under a microscope for red fluorescence (Fig. 1B and C). Another two mice were chosen to confirm the efficacy of orthotopic transplantation 10 days with green fluorescent protein (GFP)-labeled stem cells. GFP transfection: the cells were transfected into a medium containing GFP-lentivirus (20) and the amount of GFP-lentivirus was the MOI value found in the pre-experiment (21). The infected cells were cultured for 48 h for detection and transplantation. GFP-labeled BMSCs were heated at 37°C for 5 min and cooled at 4°C for 15 min, and then re-suspended in PBS (2×10^5 cells/mL). The injection method is described above.

Three experimental groups were established using 6–8-week-old male mice (n = 12) to compare the effect of BMSC transplantation: control group, mice given normal drinking water and injected PBS orthotopically; PBS group, mice treated with iodine for 12 weeks to establish the thyroiditis model and injected with PBS orthotopically; and BMSC group, mice treated with iodine for 12 weeks and transplanted with BMSCs orthotopically. The injection and transplantation methods were performed as described above; however, CM-Dil was not used to stain the transplanted cells in the BMSC group. This was conducted to mitigate the possibility that dyes and solvents could compromise the immunological response. After injection, all mice were given regular drinking water for 10 days. Mice were then sacrificed, and the cardiac blood, spleen, and thyroid glands were harvested for subsequent analyses.

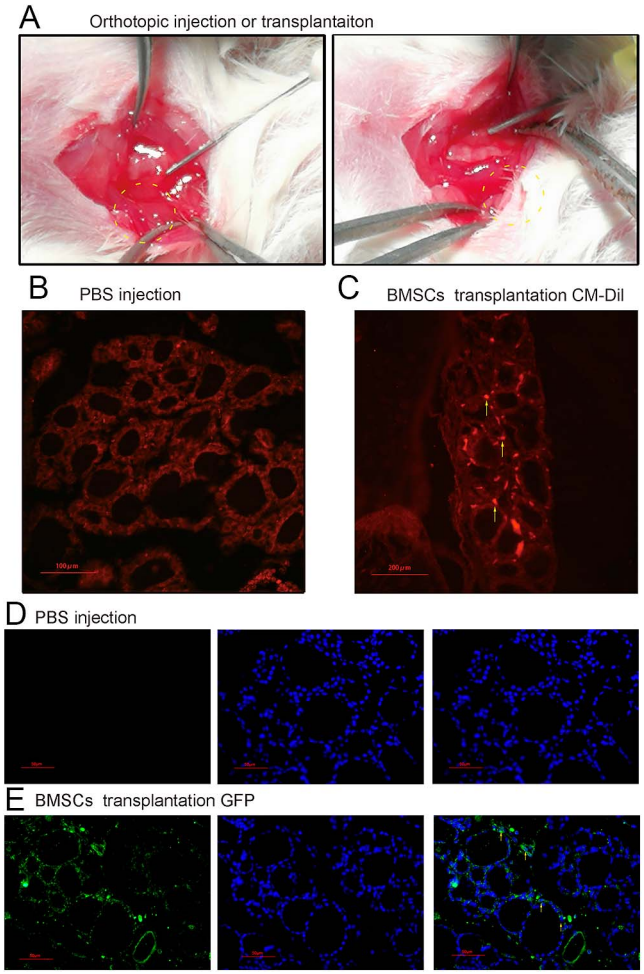

Figure 1

CM-Dil-stained BMSCs orthotopic transplanted into the thyroid gland. (A) Bone marrow mesenchymal stem cells in orthotopic injection and transplantation in the thyroid; the round yellow dotted line indicates a slight thyroid swelling after injection. (B) PBS orthotopic injection in normal mice showing no fluorescent cells. Magnification ×200, scale bars 100 μm. (C) CM-Dil-labeled BMSCs on the first day after BMSCs orthotopic transplantation, red fluorescent cells were BMSCs transplanted as the yellow arrow indicated. Magnification ×100, scale bars 200 μm. (D) PBS orthotopic injection in normal mice after 10 days showing no fluorescent cells. Magnification ×400, scale bars 50 μm. (E) GFP-labeled BMSCs on the 10th day after BMSCs orthotopic transplantation, green fluorescent cells were BMSCs transplanted as the yellow arrow indicated. Magnification ×400, scale bars 50 μm.

Hematoxylin and eosin (H and E) staining and inflammation scoring

Freshly removed thyroid glands were fixed in 4% paraformaldehyde, dehydrated using increasing ethanol gradients, cleared with xylene, and embedded in paraffin. Tissues were sectioned at 4-μm thickness and H and E staining was performed following the standard protocol. Inflammation was assessed following the International Universal NOD.H-2^{h4} mouse autoimmune thyroiditis scoring criteria (22): 0, no infiltration; 1, cell aggregation between two or more follicles in the interstitial space; 2, one or two cell foci that are at least one follicle in size; 3, widespread infiltration of 10–40% of the area; 4, extensive infiltration (between 40–80%) of the

European Thyroid Journal (2025) **14** e240137
https://doi.org/10.1530/ETJ-24-0137

territory; and 5, substantial infiltration of >80% of the area.

Enzyme-linked immunosorbent assay (ELISA)

Thyroglobulin (Tg) was extracted using the salting-out and purification method reported for Kunming mice (23). It was coated onto 96-well plates, and an indirect ELISA was used, as previously described, to determine the serum level of thyroglobulin antibody (TgAb) (23).

The levels of mouse serum thyroid stimulating hormone (TSH; Cat#CEA463Mu, Cloudclone, USA), free thyroxine (fT3; Cat#CEA186Ge, Cloudclone), and free triiodothyronine (fT4; Cat#CEA185Ge, Cloudclone) were used to assess thyroid function. The inflammation-related cytokines in the cardiac blood of mice (including tumor necrosis factor-alpha (TNF-α; Cat#EK0527, Boster, China), interferon-gamma (IFN-γ; Cat#EK0375, Boster), TGF-β (Cat#EK0515, Boster), and interleukin-10 (IL-10; Cat#EK0417, Boster)) were determined using ELISA kits following the manufacturer's instructions.

Immunohistochemistry and Western blot

Thyroid gland sections (4 μm) underwent routine clearance with xylene, rehydration with a decreasing ethanol gradient, and inactivation of endogenous peroxidase activity with 3% H_2O_2 over 2–8 h at 60°C. Antigen retrieval was performed by boiling the sections for 4 min in citrate buffer (pH 6.0). Sections were incubated with rabbit antibodies against proliferating cell nuclear antigen (PCNA; 1:100; Cat#ab92552, Abcam), caspase 3 (1:200; Cat#EPR18297, Abcam) and cleaved caspase-3 (1:200; Cat#EPR21032, Abcam) at 4°C overnight to identify proliferative and apoptotic cells, respectively. After washing, sections were incubated with goat anti-rabbit secondary antibodies and horse radish peroxidase at 37°C for 30 min and developed with 0.02% 3,3′-diamino-benzidine-4-HCl. The positive cells' integral optical density (IOD) in each section was measured using the Image-pro-plus 6.0 software. Proteins were extracted from thyroid tissue using the BCA Protein Assay Kit (Beyotime, China). These proteins were then subjected to SDS-PAGE electrophoresis and subsequently transferred to polyvinylidene difluoride (PVDF) membranes. The membranes were incubated with primary antibodies, followed by incubation with secondary antibodies. Finally, chemiluminescent (ECL) detection was performed to analyze the protein expression.

Flow cytometry

Freshly harvested mouse spleens were ground on a 200-mesh copper filter to prepare single-cell suspensions. Cells were incubated in RPMI 1640 medium (Hyclone) supplemented with 10% FBS, 1% penicillin/streptomycin, and 2 μL cell activation cocktail (Cat#423301, Biolegend, USA) for 6–8 h. The cells were stained with different combinations of fluorescence-conjugated antibodies (Biolegend) for different cell populations: T-helper 1 (Th1) cells, CD3+ (Cat#100218, Percp), CD4+ (Cat#100405, FITC), and IFN-γ+ (Cat#505808, PE); Th2 cells, CD3+ (Percp), CD4+ (FITC), and IL4+ (Cat#504105, PE); Th17 cells, CD3+ (Percp), CD4+ (FITC), and IL-17+ (Cat#512306, PE); and regulatory T cells (Tregs), CD4+ (FITC), CD25+ (Cat#102027 Percp), and FOXP3 + (Cat#126403, PE). Surface marker CD3, CD4, and CD25 staining was performed first. The cells were fixed and permeabilized using a kit (Cat#421002, Biolegend), and incubated with antibodies against IFN-γ, IL-4, IL-17, and FOXP3 for 30 min at 4°C in the dark. After washing with permeabilization buffer, staining buffer was used to reconstitute the suspension for analysis. Stained cells were detected using a FACSCalibur™ flow cytometer (Becton Dickinson Biosciences, USA) and analyzed using the FlowJo 7.6.1. (USA). The CD3/lymphocyte, CD4/CD3, Th1/Th2, and Th17/Treg ratios were calculated.

Double immunofluorescence staining

Rehydration and antigen retrieval from paraffin-embedded sections of the mouse thyroid was performed as described above. The sections were incubated with anti-CD90 goat (1:300; Santa Cruz) and anti-S100A4 rabbit (1:200; Cat#13018, Cell Signal Technology, USA) or anti-thyroid transcription factor-1 (TTF-1) rabbit (1:100; Cat#13018, Abcam) antibodies overnight at 4°C. The sections were then incubated with corresponding secondary antibodies, including Alexa Fluor® 488-conjugated donkey polyclonal secondary antibodies to rabbit IgG (1:1,000; Cat#ab150073, Abcam), Alexa Fluor® 488-conjugated IgG (1:1,000; Cat#ab150177, Abcam), Alexa Fluor® 594-conjugated IgG (1:1,000; Cat#ab150132, Abcam), or Alexa Fluor® 594-conjugated IgG (1:1,000; Cat#ab150084, Abcam). After washing with PBS, DAPI antifade reagent (Beyotime Biotechnology, China) was added to each sample for nuclear staining. Three distinct fields of view were tallied for the quantification of double-positive cells. The average value was calculated, and the GraphPad Prism version 8.0 (GraphPad Software, USA) was used for analysis.

Statistical analysis

The outcomes are expressed as the average ±standard deviation. The GraphPad Prism version 8.0 was used to conduct statistical analyses. Tukey's multiple comparison tests were used after a one-way analysis of variance to statistically compare the means of each column with no matching values. Values were considered significant when $P < 0.05$.

European Thyroid Journal (2025) **14** e240137
https://doi.org/10.1530/ETJ-24-0137

Results

Bone marrow mesenchymal stem cell confirmation and differentiation

Cell morphology was observed and surface marker identification was performed to verify MSCs. The extracted primary cells formed colonies or single cells after the first medium exchange 24 h after plating. On day 5 of culture, the cells covered 60% of the culture flask. The cells became long, with elliptical nuclei showing a spindle and fibroblast-like morphology. The cells achieved 80–90% confluence at day 10. Passage-1 cells gradually differentiated into uniform spindle cells with increased cell volume (Fig. 2A). Flow cytometry revealed that the $CD90^+$/ $CD73^+$/ $CD105^+$/$CD34^-$ phenotype was consistent with the surface antigen expression of MSCs (Fig. 2B) (24).

Induction culture was used to verify the differentiation of BMSCs. The 21-day osteoblast-induced culture contained calcium nodules, stained with alizarin red (Fig. 2C, left panel). The 14-day adipogenic cell-induced culture contained fat granules, stained with Oil red O (Fig. 2C, middle panel), and the 21-day chondrocyte-induced culture contained chondrocytes, stained with toluidine blue (Fig. 2C, right panel). Thus, surface marker expression and differentiation capacity confirmed the successful isolation of BMSCs suitable for transplantation.

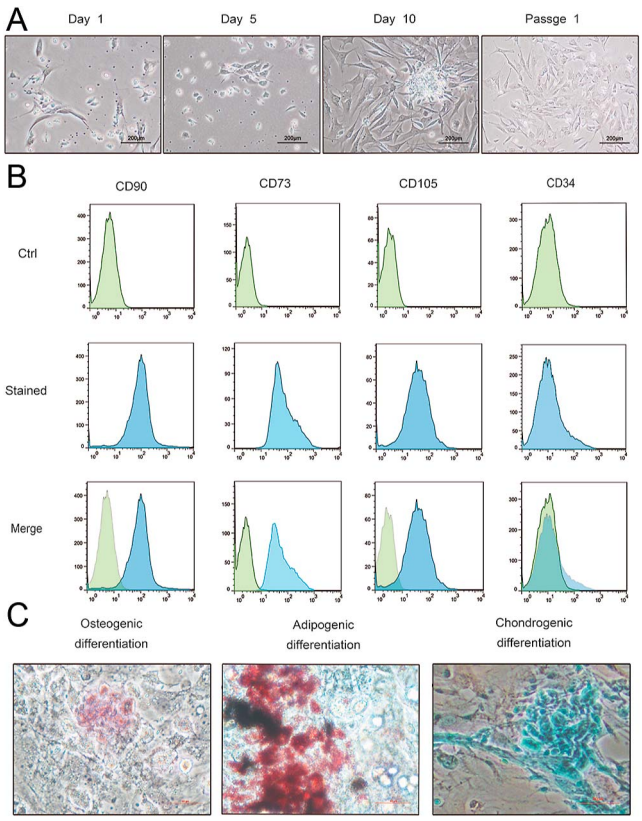

Figure 2

Identifying an induction culture of bone marrow-derived mesenchymal stem cells (BMSCs). (A) The morphology of cultured BMSCs, Magnification ×100, scale bars 200 μm. (B) Flow cytometry showing the surface markers of BMSCs. (C) Induction culture of bone BMSCs. Magnification ×400, scale bars 50 μm. The left panel shows the osteoblasts induction culture, the middle panel shows the adipocyte induction culture and the right panel shows the chondrocyte induction culture.

Thyroiditis severity positively correlated with the duration of iodine intake

Inflammatory cell infiltration was scored on H and E stained, paraffin-embedded thyroid tissues. In control mice (normal drinking water), only a few inflammatory cells were visible in the glandular stroma of the thyroid glands. However, the degree of inflammatory cell infiltration increased proportionally with the duration of iodine treatment in the iodine-supplemented groups, with an enlarged region of inflammatory cell infiltration (Fig. 3A). The length of iodine consumption and the average inflammatory score was positively correlated. The inflammatory score was significantly lower in the 8-week group compared to the 12- and 16-week groups. In addition, one 8-week group mouse did not develop thyroiditis (score 0); however, the thyroiditis model was successfully established in all mice of the other two groups (Fig. 3B). Thus, the 12-week treatment was considered optimal for establishing a stable thyroiditis model with prominent inflammatory infiltration.

Iodine treatment increased TgAb levels with time

The TgAb level in the serum of the NOD.H-2^{h4} mice was evaluated to analyze their immune state after iodine treatment. TgAb levels were lower in the 8-week group than in the 12- and 16-week groups. Although the difference was insignificant, the average value in the 12-week group was lower than that in the 16-week group (Fig. 3C). Similar to the thyroid scores, TgAb levels increased with the duration of iodine supplementation and positively associated with thyroiditis severity (Fig. 3B and C). Serum levels of TSH, fT3, and fT4 did not significantly differ between the iodine therapy and control groups (Fig. 3D).

Bone marrow mesenchymal stem cell transplantation decreased serum TgAb levels

Almost no lymphocyte infiltration was detected in the thyroid of the normal drinking water group. However, both groups supplemented with iodine showed infiltrating cells according to H and E staining (Fig. 4A and B). The average inflammatory score of the BMSC group was lower than that of the PBS group, although it was not statistically significant. TgAb levels were

European Thyroid Journal (2025) **14** e240137
https://doi.org/10.1530/ETJ-24-0137

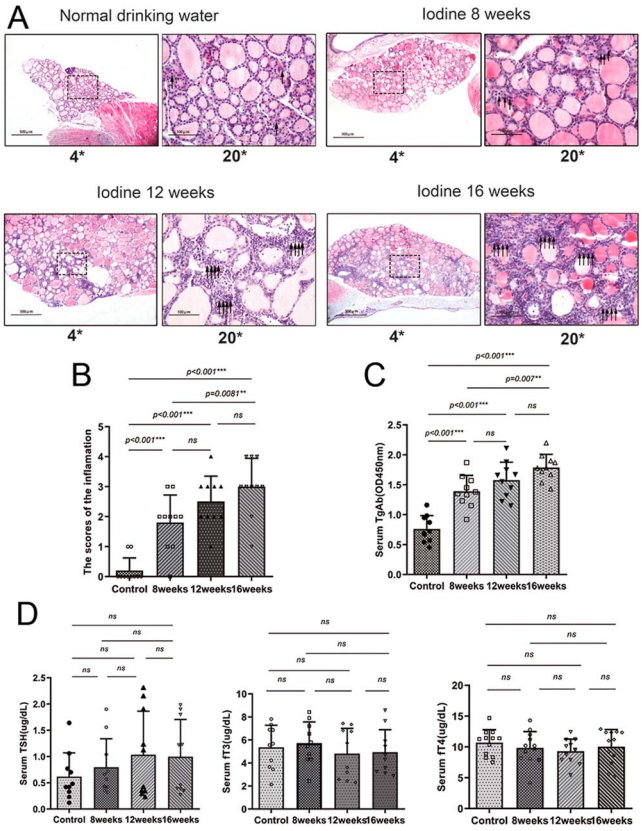

Figure 3

Establishing the thyroiditis model and inflammation scores of different iodine groups. (A) Hematoxylin and eosin (H and E) staining of different iodine groups, with infiltrating cells indicated as a black arrow. Magnification ×40 and ×200, scale bars 500 and 100 μm. (B) Inflammation scores of H and E staining of NOD.H-2^{h4} thyroiditis mice. Data are represented as the mean ± SD, n = 10 animals. One-way ANOVA was used; ns stands for not significant; *P < 0.05, **P < 0.01, ***P < 0.001. (C) Serum TgAb level of each NOD.H-2^{h4} group. Data are represented as the mean ± SD, n = 10 animals. One-way ANOVA was used; ns stands for not significant; *P < 0.05, **P < 0.01, ***P < 0.001. (D) Enzyme-linked immunosorbent assay detected the levels of serum TSH, FT3, and FT4. Data are represented as the mean ± SD, n = 10 animals. One-way ANOVA was used, ns stands for not significant.

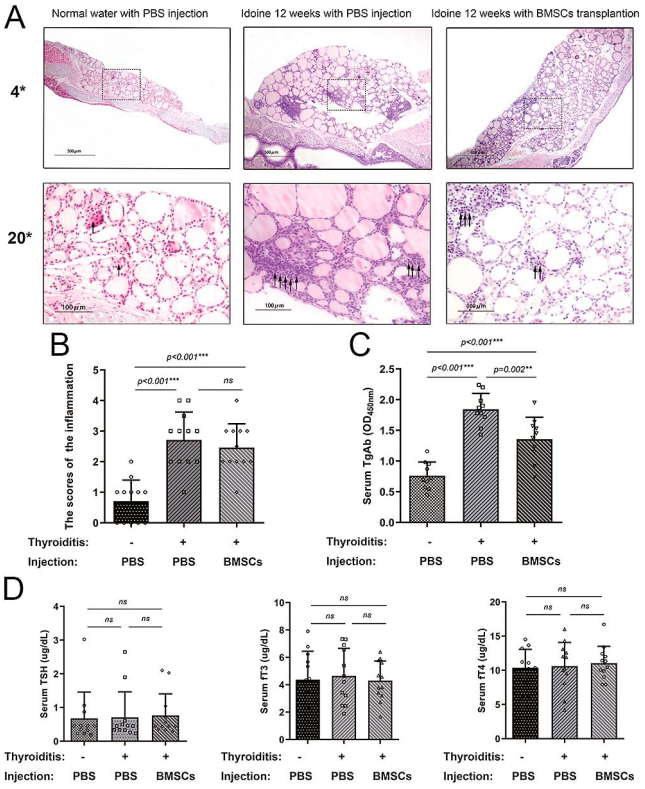

Figure 4

Bone marrow MSC transplantation decreases the serum TgAb levels without significant effects on the degree of inflammatory infiltration and thyroid function. (A) Hematoxylin and eosin staining shows the condition of the infiltrated cells in each group, with infiltrated cells indicated as the black arrow. Magnification ×40 and ×200, scale bars 500 and 100 μm. (B) Inflammatory scores of thyroiditis in each experimental group. Data are represented as the mean ± SD, n = 12 animals. One-way ANOVA was used; ns stands for not significant; ***P < 0.001. (C) Serum levels of TgAb in each experimental group. Data are represented as the mean ± SD, n = 12 animals. One-way ANOVA was used, **P < 0.01, ***P < 0.001. (D) Serum thyroid function levels in NOD.H-2^{h4} mice in each experimental group. Data are represented as the mean ± SD, n = 12 animals. One-way ANOVA was used, ns stands for not significant.

significantly lower in the BMSC group than in the PBS group (Fig. 4C). Thyroid function was not significantly different among the three groups, with similar serum levels of TSH, fT3, and fT4 (Fig. 4D).

Bone marrow mesenchymal stem cell transplantation downregulated apoptosis marker caspase 3 and upregulated proliferation marker PCNA in the thyroid tissue

Caspase 3, cleaved caspase 3 and PCNA staining were used to assess apoptosis and proliferation, respectively. Compared to the thyroiditis + PBS group, caspase 3, cleaved caspase 3 and PCNA expression significantly decreased and increased in the BMSC group, respectively (Fig. 5A, B, C, D and Fig. 6A, B, C, D, E).

Bone marrow mesenchymal stem cell transplantation decreased CD4/CD3, Th1/Th2, and Th17/Treg ratios in lymphocytes

Lymphocyte changes in splenocytes after BMSC transplantation were observed using flow cytometry. The CD4/CD3 ratio decreased in the gated mononuclear splenocytes mainly represented by lymphocytes (left panel of Fig. 7A and B); however, the CD3/ lymphocyte ratio did not significantly change (Fig. 7C and D). The immune system depends on the

European Thyroid Journal (2025) **14** e240137
https://doi.org/10.1530/ETJ-24-0137

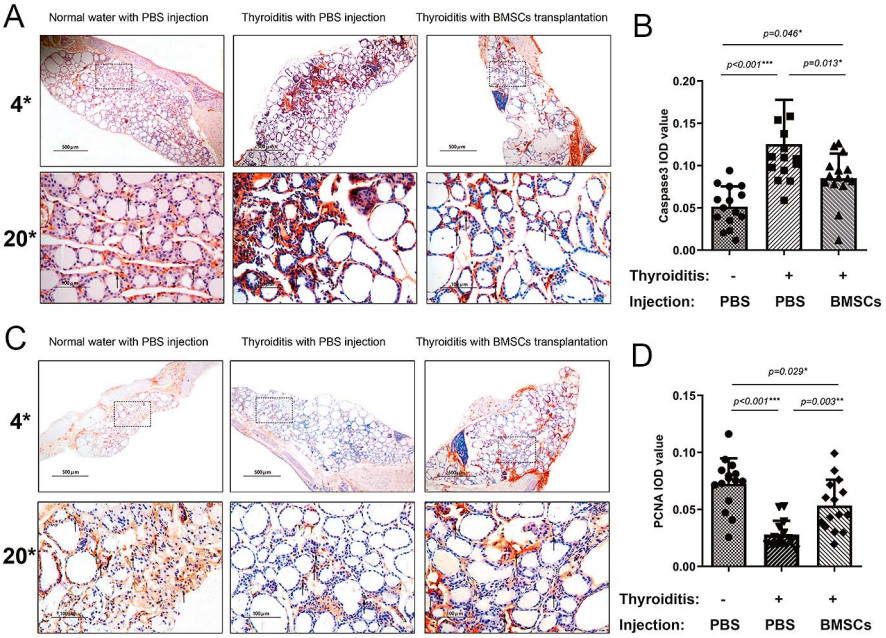

Figure 5

Immunohistochemical staining of caspase 3 and PCNA in the thyroid of each group. (A) Immunohistochemical staining of caspase 3, with infiltrating cells indicated as a black arrow. Magnification ×40 and ×200, scale bars 500 and 100 μm. (B) IOD value of staining caspase 3 in each group. Data are represented as the mean ± SD, n = 12 animals. One-way ANOVA was used, $^{*}P < 0.05$, $^{***}P < 0.001$. (C) Immunohistochemical staining of PCNA, infiltrating cells indicated as a black arrow. Magnification ×40 and ×200, scale bars 500 and 100 μm. (D) IOD value of staining PCNA in each group. Data are represented as the mean ± SD, n = 12 animals. One-way ANOVA was used, $^{*}P < 0.05$, $^{**}P < 0.01$, $^{***}P < 0.001$.

equilibrium between Th1/Th2 and Th17/Treg cells; higher ratios indicate more severe autoimmune thyroiditis. A significantly lower Th1/Th2 ratio was observed in the BMSC group, indicating a reduced autoimmune inflammation (Fig. 7A and E). Similarly, the Th17/Treg ratio significantly decreased in the BMSC group (Fig. 7B and F).

Bone marrow mesenchymal stem cell transplantation reduced proinflammatory and promoted suppressive inflammatory cytokine levels in peripheral blood

Cytokine levels in peripheral blood were measured to evaluate inflammation in NOD.H-2^{h4} mice with transplanted BMSCs. Proinflammatory cytokines TNF-α and IFN-γ were lower in the BMSC group than in the PBS group (Fig. 7G and H). However, the levels of TGF-β and IL-10 were higher in the BMSC group than in the PBS group (Fig. 7I and J).

Bone marrow mesenchymal stem cell transplantation increased co-expression of CD90/S100A4 and CD90/TTF-1

Cell differentiation and variation after BMSC transplantation were evaluated using immunofluorescence staining. Double staining of CD90 (membrane protein of cell interaction and surface marker of MSCs) and S100A4 (surface marker of fibroblasts) was performed to detect the proliferation of fibroblasts after BMSC transplantation. The number of double-positive CD90 and S100A4 cells increased after BMSC transplantation (Fig. 8A and B). Double staining of CD90 and TTF-1 (surface marker of thyrocytes) increased after BMSC transplantation (Fig. 8C and D).

Discussion

Iodine is essential for synthesizing thyroid hormones and is a key component of Tg. However, epidemiological studies suggest that excessive iodine intake can cause or exacerbate autoimmune thyroid diseases. Excess iodine combines with Tg and induces exposure of the self-epitope in the thyroid. T lymphocytes recognize the exposed autoantigens and activate an inflammatory response, leading to autoimmune thyroiditis (25, 26).

In the short-term, increased sensitivity to Tg injections orthotopically into the thyroid causes EAT. However, these animals do not have a susceptible genetic background, and the models do not reflect the pathogenesis of iodine intake (27). We established a model for autoimmune thyroiditis using iodine induction in NOD.H-2^{h4} mice with the susceptibility gene H-2 to recognize overexposure to the autoantigen Tg under the simulation of iodine intake. Consistent with the pathogenesis of autoimmune thyroiditis and HT in humans (18), the inflammatory response of the thyroid in our model increased with the duration of iodine intake. The elevated levels of TgAb prove their consistency with earlier studies (28).

Regarding the evaluation of stem cell quality, although we did not detect repressor/activator protein 1 (RAP1) (29) in the experiment to assess their senescence status, we observed and controlled the state and quality of the cells during cell culture and passage. Generally, senescent cells exhibit a gradual flattening and

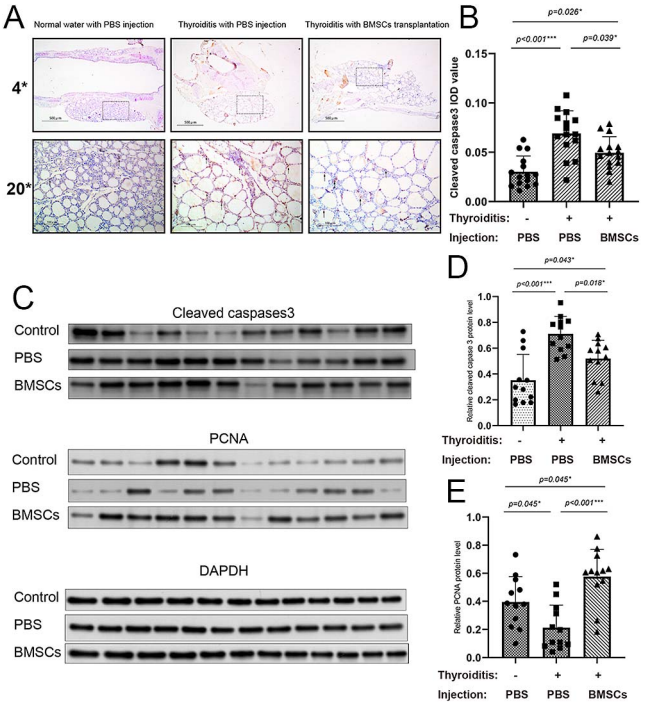

Figure 6

Immunohistochemical staining and western blot of cleaved caspase 3 and PCNA in the thyroid of each group. (A) Immunohistochemical staining of cleaved caspase 3, with infiltrating cells indicated as a black arrow. Magnification ×40 and ×200, scale bars 500 and 100 μm. (B) IOD value of staining cleaved caspase 3 in each group. Data are represented as the mean ± SD, n = 12 animals. One-way ANOVA was used, $^{*}P < 0.05$, $^{***}P < 0.001$. (C) Western blot of cleaved caspase 3 and PCNA. (D) and (E) Relative level of cleaved caspase 3 and PCNA in each group. Data are represented as the mean ± SD, n = 12 animals. One-way ANOVA was used, $^{*}P < 0.05$, $^{**}P < 0.01$, $^{***}P < 0.001$.

hypertrophy of the cell morphology, with more granular substances appearing in the cytoplasm, and a decrease in proliferation and differentiation capabilities (30). In Fig. 2A, on day 10, the number of flat cells increased, but new cells and cell growth centers were still visible. After passage (Fig. 2A – passage 1), the number of flat and enlarged cells decreased, while the number of mature cells with a rod-like shape increased, and small cells that were growing and had just divided were still visible, and the cells could still be passed. At the same time, in the differentiation experiment (Fig. 3C), their differentiation ability was confirmed. Through the above experiments and observations, we confirmed that the P1 generation cells we cultivated were of acceptable quality and could be used.

Under inflammation and damage conditions, MSCs exhibit strong immunomodulatory and tissue repair effects. MSCs mainly function through intercellular contact and paracellular secretion of immunoregulatory cytokines, such as TGF-β1, PGE2, IDO, and IL-10, and assist in repairing local and systemic immune impairments and tissue damage (5, 6, 7). Our results showed that the average CD4 percentage was low, such as the decreased TgAb levels, suggesting that transplanted BMSCs blocked antigen presentation, reduced T and B cell activities, induced M1 macrophages to adopt the anti-inflammatory M2 form, and reduced B cell IgG production. Hence, the acquired and humoral immune responses of thyroiditis were alleviated (31, 32). Furthermore, the Th1/Th2 and Th17/Treg ratios significantly decreased after BMSC transplantation. This can be attributed to the secretion of regulatory cytokines by BMSCs, specifically transforming IL-10 and TGF-β. These cytokines decrease BMSC differentiation into Th1 and Th17 cells, while concurrently increasing the proportion of tolerogenic Th2 cells and Tregs (21, 33, 34). Moreover, the proinflammatory cytokines IL-1, TNF-α, and IFN-γ secreted by Th1 and Th17 cells decreased at the expense of activating cytotoxic T lymphocytes and natural killer (NK) cells, reducing the injurious effect of inflammation. The increased number of Tregs and functional recovery lead to more anti-inflammatory cytokines, improving the imbalance between Th1/Th2 and Th17/Treg and restoring a virtuous cycle (35, 36); the changes in cytokines (TNF-α, IFN-γ, TGF-β, and IL-10) levels confirmed this process. Therefore, changes in cytokine levels are a result of improvements in thyroiditis.

The role of IFN-γ in autoimmune inflammation and stem cell therapy is rather complex. On one hand, IFN-γ has a pro-inflammatory effect. It can activate immune cells such as macrophages and T cells, enhancing their phagocytic ability and killing function and promoting the occurrence and development of inflammatory responses. It can also induce the production of various inflammatory factors, such as IL-6, IL-12, and TNF-α, further amplifying the inflammatory response and causing tissue damage, thereby aggravating autoimmune reactions. On the other hand, IFN-γ also has an anti-inflammatory effect. IFN-γ can also regulate the differentiation and function of immune cells, induce immune tolerance, and inhibit the activity of autoreactive T cells, alleviating autoimmune inflammation (37). IFN-γ is a key inducer of the immunosuppressive function of MSCs. By activating the JAK-STAT signaling pathway, it upregulates the expression of immunosuppressive molecules (such as IDO and PD-L1) (38). In stem cell therapy, a certain level of IFN-γ is conducive to the immune regulatory function of MSCs.

Although inflammatory cell infiltration did not significantly change, inflammatory cell activity and toxic effects decreased and the thyroid tissue began to recover (7, 39). The expression of caspase 3 (apoptotic marker) decreased and PCNA (proliferation marker) increased. MSCs exert regulatory effects via the TLR4-ERK1/2-Fas/FasL-caspase 3 pathway to block apoptosis progression (40). Meanwhile, MSC can also

European Thyroid Journal (2025) **14** e240137
https://doi.org/10.1530/ETJ-24-0137

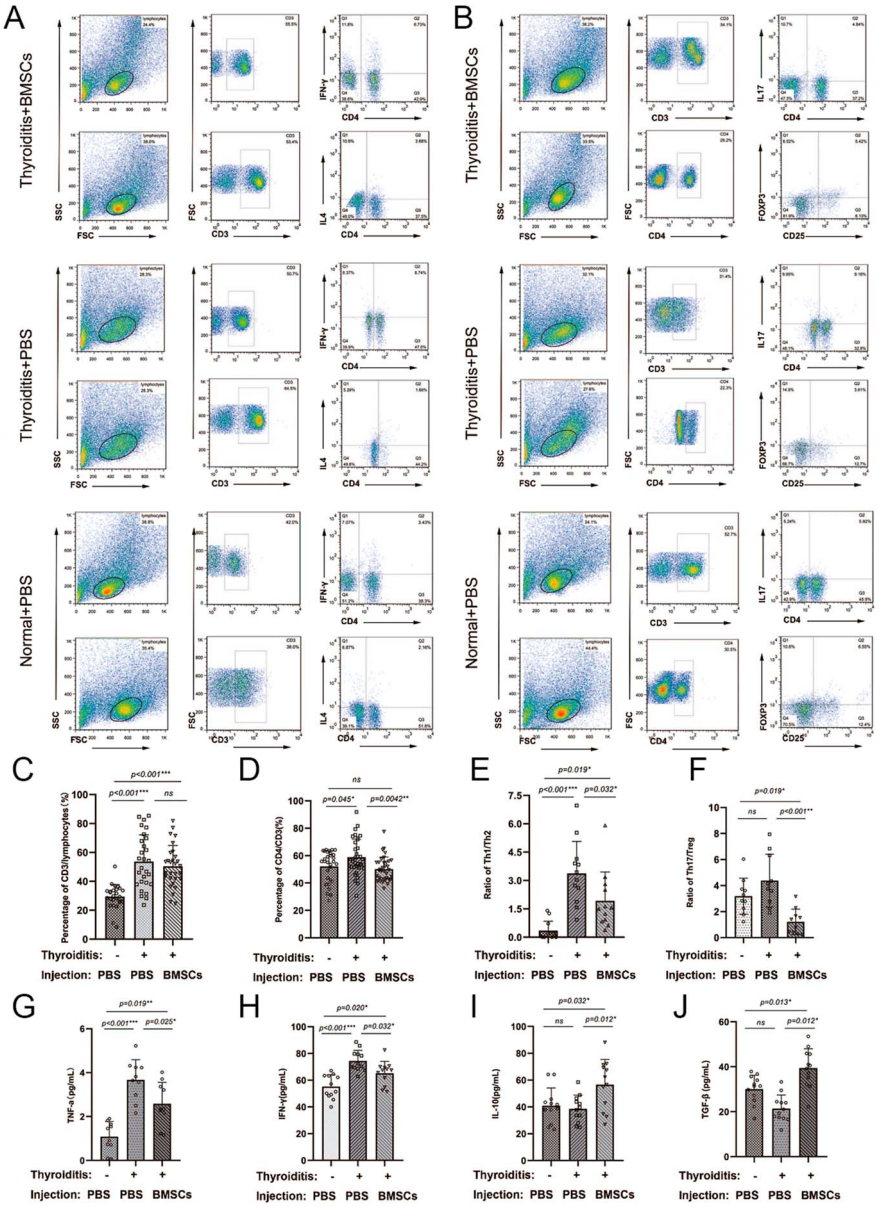

Figure 7

Proportions of lymphocytes from splenocytes were analyzed by flow cytometry and the change of cytokines in peripheral blood after BMSC transplantation. (A) The proportion of CD4, Th1 and Th2 cells in the lymphocytes was mainly shown in each group determined by flow cytometry. (B) The proportion of CD3, CD4, Th17, and Treg cells was mainly shown in each group. (c) Quantification of CD3/lymphocytes: figure (A) middle panels value averaged in each group. Data are represented as the mean ± SD, n = 12 animals. One-way ANOVA was used; ns stands for not significant, ***P < 0.001. (D) Quantification of CD4/CD: figure (B) middle panels $^{down}/_{up}$ value averaged in each group. Data are represented as the mean ± SD, n = 12 animals. One-way ANOVA was used; ns stands for not significant; *P < 0.05, **P < 0.01. (E) Quantification of Th1/Th2: figure (A) left panels $^{up\ Q2}/_{down\ Q2}$ value averaged in each group. Data are represented as the mean ± SD, n = 12 animals. One-way ANOVA was used *P < 0.05, ***P < 0.001. (F) Quantification of Th17/Tregs: figure (B) left panels $^{up\ Q2/(Q2+Q3)}/_{down\ Q2}$ value averaged in each group. Data are represented as the mean ± SD, n = 12 animals. One-way ANOVA was used; ns stands for not significant; *P < 0.05, **P < 0.01. (G, H, I, J) TNF-α, IFN-γ, IL-10, and TGF-β levels in each experimental group. Data are represented as mean ± SD, n = 12 animals. One-way ANOVA was used; ns stands for not significant; *P < 0.05, **P < 0.01, ***P < 0.001.

simultaneously inhibit the expression of cleavage of caspase 3, which is correlated with reduced Th1/Th2 responses and enhanced Treg activity (41). Following hepatic ischemia-reperfusion injury in pigs, the transplantation of stem cells resulted in an upregulation of PCNA expression, thereby facilitating liver tissue regeneration (42).

In our study, iodine intake did not affect thyroid function. TSH, fT3, and fT4 serum levels were similar across the treatment groups, possibly owing to the short duration of iodine treatment; therefore, the follicular structure within the thyroid of the mice could still exert its compensatory effect to maintain normal thyroid function under the excessive immune response (43, 44). In NOD.H-2^{h4} mice, autoimmune thyroiditis rarely progresses to hypothyroidism (43). In humans, noticeable changes in thyroid function may take years or even decades (2), and mice may require extended iodine intake to adequately mimic the human condition.

Thyroid peroxidase antibody (TPOAb) is another important evaluation indicator for HT and its expression correlates with TSH level and the degree of thyroid cell destruction (2). TPOAb detection is easy in humans and difficult in mice (45). In addition, TPOAb develops later than TgAb in mice (46). Therefore, TgAbs are preferred for mouse thyroiditis experiments (43, 46). Nevertheless, the trend of TPOAb expression in NOD.H-2^{h4} mice with autoimmunity-related thyroiditis is generally the same as that of TgAb (46).

European Thyroid Journal (2025) **14** e240137
https://doi.org/10.1530/ETJ-24-0137

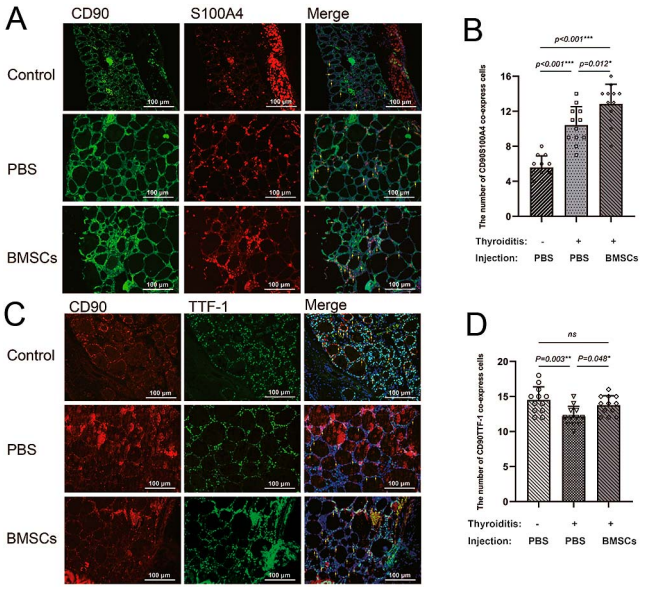

Figure 8

Immunofluorescence double staining of CD90/S100A4 and CD90/TTF-1. (A) CD90 and S100A4 double staining, the double-positive cells indicated as a yellow arrow. Magnification ×200, scale bars 100 μm. (B) Quantification of CD90 and S100A4 dual stain positive cells. Data are represented as the mean ± SD, $n = 12$ animals. One-way ANOVA was used, $^{**}P < 0.01$, $^{***}P < 0.001$. (C) CD90 and TTF-1 double staining, the double-positive cells indicated as the yellow arrow. Magnification ×200. (D) Quantification of CD90 and S100A4 dual stain positive cells. Data are represented as the mean ± SD, $n = 12$ animals. One-way ANOVA was used; ns stands for not significant; $P < 0.05$*, $^{**}P < 0.01$.

Although research has noted therapeutic effects of MSCs, few have focused on the changes the cells undergo after transplantation *in vivo*. We characterized the variation in BMSCs after injection to interpret their functions and effects indirectly. CD90 (Thy1) is a GPI-anchored development regulatory protein and receptor or integrin ligand that mediates cell–cell and cell–matrix interactions involved in the signaling cascades of cellular adhesion, migration, neurite outgrowth, tumor growth, and fibrosis. CD90 is abundantly expressed in a subset of fibroblasts, endothelial cells, and hematopoietic cells and is one of the first surface markers identified on MSCs; CD90+ cells are more likely to originate from mesenchymal cells, MSC and the intertransformation process between mesenchymal cells and epithelial cells (47, 48). In this study, CD90 was used in our study to show the effect of transplanted BMSCs on the tissue *in situ*. S100A4 is a fibroblast marker involved in cytoskeletal dynamics and cell movement (49). The co-expression of CD90 and S100A4 indicates that active fibroblasts regulated fibrosis. CD90+ fibroblasts can promote the differentiation of myofibroblasts, mediate tissue contraction and repair after injury, and alleviate fibrotic damage in pulmonary fibrosis (50, 51). Our results suggested that more fibroblasts were produced in tissues with thyroiditis, and the increased co-expression of CD90 and S100A4 suggested that BMSC treatment promoted thyroid tissue repair. Moreover, our results suggested that there is also a possibility that transplanted BMSCs may transform into fibroblasts.

TTF-1 is a homologous transcription factor from the NKX family and a biomarker of thyrocytes (52); its co-expression with CD90 suggests thyrocyte development. According to our results, due to the effects of thyroiditis and injection injury, the number of double-positive cells in CD90 and TTF-1 in the PBS group decreased due to the destruction of injection injury and thyroiditis, and the recovery ability of tissue decreased. After injection of PBS, the recovery ability of interstitial and epithelial cells was improved, and inflammatory factors may still exist. Therefore, CD90 and TTF-1 double-positive cells were similar to those in the control group, but there was no significant difference. In addition, the transplanted BMSCs improved the inflammatory and damaging environment and also had the potential to differentiate into thyroid cells. In some environments, MSCs can differentiate into endoderm-derived pancreatic and liver cells. The ability of MSCs to differentiate into thyroid cells has not been proven *in vivo* or *in vitro* (53, 54). Cell fusion is a form of cell transformation. MSCs form multicellular aggregates interacting with neighboring cells, showing common characteristic features with fused genetic information (55). The MSC fusion mechanism is involved in ameliorating neurodegenerative diseases and treating gastrointestinal epithelial lesions (56, 57). Although we noticed a rise in the co-expression of CD90 and TTF-1, further experiments are needed to clarify the variations in MSCs and fibroblasts in thyroid tissues.

We explored the effect of the delivery route on the efficacy of BMSC treatment. Although orthotopic transplantation may cause certain local injuries, it is more effective than caudal intravenous injection (17, 18). In addition, 0.1–2.7% of cells administered via caudal intravenous injection make it to the local lesions and most are found in the lungs (58, 59). Therefore, better therapeutic effects can be obtained by improving the heterogeneity of the cells, adjusting the number of transplanted cells, or using them in orthotopic and intravenous combinations.

Orthotopic injection of BMSCs into the thyroid exhibited favorable therapeutic efficacy in NOD.H-2^{h4} mice suffering from thyroiditis caused by iodine-induced autoimmunity via regulating the immune system, suppressing cell apoptosis, and promoting the regeneration of cells in the thyroid tissue. In addition, transplanted BMSCs can potentially transform into fibroblasts and thyroid cells. Optimizing the transplantation settings may maximize BMSC therapeutic effects, providing a promising clinical translation strategy for treating HT. This study elucidated the pathogenesis of HT and provided evidence supporting the potential of BMSCs in HT treatment.

Declaration of interest

The authors declare that there is no conflict of interest that could be perceived as prejudicing the impartiality of the work reported.

Funding

This work was supported by the National Natural Science Foundation of China (grant number 81600602) and Liaoning Provincial Science and Technology Plan Joint Program (2024-MSLH-583).

Author contribution statement

X Liu helped in writing of the original draft. L Cui and Y Han helped in formal analysis. J Dong helped in investigation. J Ren helped in investigation and data curation. D Xu and J Zhang helped in conceptualization.

Data availability

The study's supporting data can be accessed upon request from the corresponding author.

Ethics approval and consent to participate

The animal husbandry practices and experimental procedures followed all necessary standards and were conducted with the approval of the Institutional Animal Care and Use Committee (IACUC) at China Medical University.

Acknowledgments

We acknowledge the helpful suggestions and encouragement from the staff, especially Professor Yuchen Han at the Institute of Pathology of China Medical University. We also express our gratitude to the dedicated individuals in the Department of Vascular and Thyroid Surgery at the First Hospital of China Medical University.

References

1 Ahmed R, Al-Shaikh S & Akhtar M. Hashimoto thyroiditis: a century later. *Adv Anat Pathol* 2012 **19** 181–186. (https://doi.org/10.1097/pap.0b013e3182534868)

2 Caturegli P, De Remigis A & Rose NR. Hashimoto thyroiditis: clinical and diagnostic criteria. *Autoimmun Rev* 2014 **13** 391–397. (https://doi.org/10.1016/j.autrev.2014.01.007)

3 Tomer Y & Huber A. The etiology of autoimmune thyroid disease: a story of genes and environment. *J Autoimmun* 2009 **32** 231–239. (https://doi.org/10.1016/j.jaut.2009.02.007)

4 Teng W, Shan Z, Teng X, *et al.* Effect of iodine intake on thyroid diseases in China. *N Engl J Med* 2006 **354** 2783–2793. (https://doi.org/10.1056/nejmoa054022)

5 Uccelli A, Moretta L & Pistoia V. Mesenchymal stem cells in health and disease. *Nat Rev Immunol* 2008 **8** 726–736. (https://doi.org/10.1038/nri2395)

6 Liu S, Liu F, Zhou Y, *et al.* Immunosuppressive property of MSCs mediated by cell surface receptors. *Front Immunol* 2020 **11** 1076. (https://doi.org/10.3389/fimmu.2020.01076)

7 Vasanthan J, Gurusamy N, Rajasingh S, *et al.* Role of human mesenchymal stem cells in regenerative therapy. *Cells* 2020 **10** 54. (https://doi.org/10.3390/cells10010054)

8 Castro-Manrreza ME & Montesinos JJ. Immunoregulation by mesenchymal stem cells: biological aspects and clinical applications. *J Immunol Res* 2015 **2015** 394917. (https://doi.org/10.1155/2015/394917)

9 Muroi K, Miyamura K, Ohashi K, *et al.* Unrelated allogeneic bone marrow-derived mesenchymal stem cells for steroid-refractory acute graft-versus-host disease: a phase I/II study. *Int J Hematol* 2013 **98** 206–213. (https://doi.org/10.1007/s12185-013-1399-4)

10 Llufriu S, Sepulveda M, Blanco Y, *et al.* Randomized placebo-controlled phase II trial of autologous mesenchymal stem cells in multiple sclerosis. *PLoS One* 2014 **9** e113936. (https://doi.org/10.1371/journal.pone.0113936)

11 Forbes GM, Sturm MJ, Leong RW, *et al.* A phase 2 study of allogeneic mesenchymal stromal cells for luminal Crohn's disease refractory to biologic therapy. *Clin Gastroenterol Hepatol* 2014 **12** 64–71. (https://doi.org/10.1016/j.cgh.2013.06.021)

12 Álvaro-Gracia JM, Jover JA, García-Vicuña R, *et al.* Intravenous administration of expanded allogeneic adipose-derived mesenchymal stem cells in refractory rheumatoid arthritis (Cx611): results of a multicentre, dose-escalation, randomized, single-blind, placebo-controlled phase Ib/IIa clinical trial. Intravenous administration of expanded allogeneic adipose-derived mesenchymal stem cells in refractory rheumatoid arthritis (Cx611): results of a multicentre, dose-escalation, randomized, single-blind, placebo-controlled phase Ib/IIa clinical trial. *Ann Rheum Dis* 2017 **76** 196–202. (https://doi.org/10.1136/annrheumdis-2015-208918)

13 Goodwin M, Sueblinvong V, Eisenhauer P, *et al.* Bone marrow-derived mesenchymal stromal cells inhibit Th2-Mediated allergic airways inflammation in mice. *Stem Cell* 2011 **29** 1137–1148. (https://doi.org/10.1002/stem.656)

14 Zhang Q, Shi S, Liu Y, *et al.* Mesenchymal stem cells derived from human gingiva are capable of immunomodulatory functions and ameliorate inflammation-related tissue destruction in experimental colitis. *J Immunol* 2009 **183** 7787–7798. (https://doi.org/10.4049/jimmunol.0902318)

15 Zappia E, Casazza S, Pedemonte E, *et al.* Mesenchymal stem cells ameliorate experimental autoimmune encephalomyelitis inducing T-cell anergy. *Blood* 2005 **106** 1755–1761. (https://doi.org/10.1182/blood-2005-04-1496)

16 Chang J-W, Hung S-P, Wu H-H, *et al.* Therapeutic effects of umbilical cord blood-derived mesenchymal stem cell transplantation in experimental lupus nephritis. *Cell Transplant* 2011 **20** 245–257. (https://doi.org/10.3727/096368910x520056)

17 Choi EW, Shin IS, Lee HW, *et al.* Transplantation of CTLA4Ig gene-transduced adipose tissue-derived mesenchymal stem cells reduces inflammatory immune response and improves Th1/Th2 balance in experimental autoimmune thyroiditis. *J Gene Med* 2011 **13** 3–16. (https://doi.org/10.1002/jgm.1531)

18 Choi EW, Lee JM, Lee HW, *et al.* Therapeutic effects of CTIA4Ig gene-transduced adipose tissue-derived mesenchymal stem cell transplantation on established autoimmune thyroiditis. *Cell Transplant* 2015 **24** 2221–2236. (https://doi.org/10.3727/096368914x685122)

19 Zhu H, Guo Z-K, Jiang X-X, *et al.* A protocol for isolation and culture of mesenchymal stem cells from mouse compact bone. *Nat Protoc* 2010 **5** 550–560. (https://doi.org/10.1038/nprot.2009.238)

20 Jiang D, Gao F, Zhang Y, *et al.* Mitochondrial transfer of mesenchymal stem cells effectively protects corneal epithelial cells from mitochondrial damage. *Cell Death Dis* 2016 **7** e2467. (https://doi.org/10.1038/cddis.2016.358)

21 Ren G, Zhang L, Zhao X, *et al.* Mesenchymal stem cell-mediated immunosuppression occurs via concerted action of chemokines and nitric oxide. *Cell Stem Cell* 2008 **2** 141–150. (https://doi.org/10.1016/j.stem.2007.11.014)

22 Kolypetri P, Carayanniotis K, Rahman S, *et al.* The thyroxine-containing thyroglobulin peptide (aa 2549-2560) is a target epitope in iodide-accelerated spontaneous autoimmune thyroiditis. *J Immunol* 2014 **193** 96–101. (https://doi.org/10.4049/jimmunol.1400561)

23 Xiaochun T, Xiukun JIA, Chenling F, *et al*. Extraction purification and identification thyroglobulin of mouse. *China J Madern Med* 2007 **17** 1467–1469. (https://doi.org/10.3969/j.issn.1005-8982.2007.12.016)

24 Dominici M, Le Blanc K, Mueller I, *et al.* Minimal criteria for defining multipotent mesenchymal stromal cells. The international society for cellular therapy position statement. *Cytopathology* 2006 **8** 315–317. (https://doi.org/10.1080/14653240600855905)

25 Allen EM, Appel MC & Braverman LE. The effect of iodide ingestion on the development of spontaneous lymphocytic thyroiditis in the diabetes-prone bb/w rat. *Endocrinology* 1986 **118** 1977–1981. (https://doi.org/10.1210/endo-118-5-1977)

26 Champion BR, Page KR, Parish N, *et al.* Identification of a thyroxine-containing self-epitope of thyroglobulin which triggers thyroid autoreactive t-cells. *J Exp Med* 1991 **174** 363–370. (https://doi.org/10.1084/jem.174.2.363)

27 Lam-Tse WK, Lernmark A & Drexhage HA. Animal models of endocrine/organ-specific autoimmune diseases: do they really help us to understand human autoimmunity? *Springer Semin Immunopathol* 2002 **24** 297–321. (https://doi.org/10.1007/s00281-002-0110-2)

28 Teng X, Shan Z, Teng W, *et al.* Experimental study on the effects of chronic iodine excess on thyroid function, structure, and autoimmunity in autoimmune-prone NOD.H-2h4 mice. *Clin Exp Med* 2009 **9** 51–59. (https://doi.org/10.1007/s10238-008-0014-0)

29 Poon MW, Yan L, Jiang D, *et al.* Inhibition of RAP1 enhances corneal recovery following alkali injury. *Investig Ophthalmol Vis Sci* 2015 **56** 711–721. (https://doi.org/10.1167/iovs.14-15268)

30 Zhou X, Hong Y, Zhang H, *et al.* Mesenchymal stem cell senescence and rejuvenation: current status and challenges. *Front Cell Dev Biol* 2020 **8** 364. (https://doi.org/10.3389/fcell.2020.00364)

31 Rosado MM, Bernardo ME, Scarsella M, *et al.* Inhibition of B-Cell proliferation and antibody production by mesenchymal stromal cells is mediated by T cells. *Stem Cell Dev* 2015 **24** 93–103. (https://doi.org/10.1089/scd.2014.0155)

32 Duffy MM, Ritter T, Ceredig R, *et al.* Mesenchymal stem cell effects on T-cell effectorpathways. *Stem Cell Res Ther* 2011 **2** 34. (https://doi.org/10.1186/scrt75)

33 Aggarwal S & Pittenger MF. Human mesenchymal stem cells modulate allogeneic immune cell responses. *Blood* 2005 **105** 1815–1822. (https://doi.org/10.1182/blood-2004-04-1559)

34 Shi Y, Su J, Roberts AI, *et al.* How mesenchymal stem cells interact with tissue immune responses. *Trends Immunol* 2012 **33** 136–143. (https://doi.org/10.1016/j.it.2011.11.004)

35 Duffy MM, Ritter T, Ceredig R, *et al.* Mesenchymal stem cell effects on T-cell effector pathways. *Stem Cell Res Ther* 2011 **2** 34. (https://doi.org/10.1186/scrt75)

36 Ghannam S, Pene J, Torcy-Moquet G, *et al.* Mesenchymal stem cells inhibit human Th17 cell differentiation and function and induce a T regulatory cell phenotype. *J Immunol* 2010 **185** 302–312. (https://doi.org/10.4049/jimmunol.0902007)

37 Ivashkiv LB. IFNγ: signalling, epigenetics and roles in immunity, metabolism, disease and cancer immunotherapy. *Nat Rev Immunol* 2018 **18** 545–558. (https://doi.org/10.1038/s41577-018-0029-z)

38 Yao M, Chen Z, He X, *et al.* Cross talk between glucose metabolism and immunosuppression in IFN-γ-primed mesenchymal stem cells. *Life Sci Alliance* 2022 **5** e202201493. (https://doi.org/10.26508/lsa.202201493)

39 Ferreira JR, Teixeira GQ, Santos SG, *et al.* Mesenchymal stromal cell secretome: influencing therapeutic potential by cellular pre-conditioning. *Front Immunol* 2018 **9** 2837. (https://doi.org/10.3389/fimmu.2018.02837)

40 Tian Y, Wang J, Wang W, *et al.* Mesenchymal stem cells improve mouse non-heart-beating liver graft survival by inhibiting kupffer cell apoptosis via TLR4-ERK1/2-Fas/FasL-caspase3 pathway regulation. *Stem Cell Res Ther* 2016 **7** 157. (https://doi.org/10.1186/s13287-016-0416-y)

41 Li CL, Leng Y, Zhao B, *et al.* Human iPSC-MSC-Derived xenografts modulate immune responses by inhibiting the cleavage of caspases. *Stem Cell* 2017 **35** 1719–1732. (https://doi.org/10.1002/stem.2638)

42 Jiao Z, Ma Y, Liu X, *et al.* Adipose-derived stem cell transplantation attenuates inflammation and promotes liver regeneration after ischemia-reperfusion and hemihepatectomy in swine. *Stem Cells Int* 2019 **2019** 2489584. (https://doi.org/10.1155/2019/2489584)

43 Braley-Mullen H & Yu S. NOD.H-2h4 mice: an important and underutilized animal model of autoimmune thyroiditis and Sjogren's syndrome. *Adv Immunol* 2015 **126** 1–43. (https://doi.org/10.1016/bs.ai.2014.11.001)

44 Rapoport B. Pathophysiology of hashimotos-thyroiditis and hypothyroidism. *Annu Rev Med* 1991 **42** 91–96. (https://doi.org/10.1146/annurev.med.42.1.91)

45 Doniach D. Humoral and genetic aspects of thyroid autoimmunity. *Clin Endocrinol Metab* 1975 **4** 267–285. (https://doi.org/10.1016/s0300-595x(75)80022-3)

46 Chen CR, Hamidi S, Braley-Mullen H, *et al.* Antibodies to thyroid peroxidase arise spontaneously with age in NOD.H-2h4 mice and appear after thyroglobulin antibodies. *Endocrinology* 2010 **151** 4583–4593. (https://doi.org/10.1210/en.2010-0321)

47 Bradley JE, Ramirez G & Hagood JS. Roles and regulation of Thy-1, a context-dependent modulator of cell phenotype. *Biofactors* 2009 **35** 258–265. (https://doi.org/10.1002/biof.41)

48 Leyton L, Díaz J, Martínez S, *et al.* Thy-1/CD90 a bidirectional and lateral signaling scaffold. *Front Cell Dev Biol* 2019 **7** 132. (https://doi.org/10.3389/fcell.2019.00132)

49 Kalluri R. The biology and function of fibroblasts in cancer. *Nat Rev Cancer* 2016 **16** 582. (https://doi.org/10.1038/nrc.2016.73)

50 Pei Y, Sherry DM & McDermott AM. Thy-1 distinguishes human corneal fibroblasts and myofibroblasts from keratocytes. *Exp Eye Res* 2004 **79** 705–712. (https://doi.org/10.1016/j.exer.2004.08.002)

51 White ES, Lazar MH & Thannickal VJ. Pathogenetic mechanisms in usual interstitialpneumonia/idiopathic pulmonary fibrosis. *J Pathol* 2003 **201** 343–354. (https://doi.org/10.1002/path.1446)

52 Boggaram V. Thyroid transcription factor-1 (TTF-1/Nkx2.1/TITF1) gene regulation in the lung. *Clin Sci* 2009 **116** 27–35. (https://doi.org/10.1042/cs20080068)

53 Battula VL, Bareiss PM, Treml S, *et al.* Human placenta and bone marrow derived MSC cultured in serum-free, b-FGF-containing medium express cell surface frizzled-9 and SSEA-4 and give rise to multilineage differentiation. *Differentiation* 2007 **75** 279–291. (https://doi.org/10.1111/j.1432-0436.2006.00139.x)

54 Brückner S, Tautenhahn HM, Winkler S, *et al.* Isolation and hepatocyte differentiation of mesenchymal stem cells from porcine bone marrow–"surgical waste" as a novel MSC source. *Transplant Proc* 2013 **45** 2056–2058. (https://doi.org/10.1016/j.transproceed.2013.01.101)

55 Eisenberg LM & Eisenberg CA. Stem cell plasticity, cell fusion, and transdifferentiation. *Birth Defects Res C Embryo Today* 2003 **69** 209–218. (https://doi.org/10.1002/bdrc.10017)

56 Kemp K, Gordon D, Wraith DC, *et al.* Fusion between human mesenchymal stem cells and rodent cerebellar purkinje cells. *Neuropathol Appl Neurobiol* 2011 **37** 166–178. (https://doi.org/10.1111/j.1365-2990.2010.01122.x)

57 Ferrand J, Noël D, Lehours P, *et al.* Human bone marrow-derived stem cells acquire epithelial characteristics through fusion with gastrointestinal epithelial cells. *PLoS One* 2011 **6** e19569. (https://doi.org/10.1371/journal.pone.0019569)

58 Chapel A, Bertho JM, Bensidhoum M, *et al.* Mesenchymal stem cells home to injured tissues when co-infused with hematopoietic cells to treat a radiation-induced multi-organ failure syndrome. *J Gene Med* 2003 **5** 1028–1038. (https://doi.org/10.1002/jgm.452)

59 Devine SM, Cobbs C, Jennings M, *et al.* Mesenchymal stem cells distribute toa wide range of tissues following systemic infusion into nonhuman primates. *Blood* 2003 **101** 2999–3001. (https://doi.org/10.1182/blood-2002-06-1830)